[Frontiers in Bioscience, Landmark, 26, 266-285, Jan 1, 2021]

Production of engineered cartilage from mesenchymal stem cell spheroids

Ha Thi-Ngan Le[1], Ngoc Bich Vu[1], Phuc Dang-Ngoc Nguyen[1], Thuy Thi-Thanh Dao[1], Xuan Hoang-Viet To[1], Phuc Van Pham[2]

[1]Stem Cell Institute, VNU-HCM University of Science, Ho Chi Minh City 800010, Viet Nam, [2]Laboratory of Stem Cell Research and Application, VNU-HCM University of Science, Ho Chi Minh City 800010, Viet Nam

TABLE OF CONTENTS

1. ABSTRACT

This study suggested a new method to produce the *in vitro* cartilage tissues by cartilage differentiation in spheroids from adipose-derived stem cells on porous scaffolds. Adipose-derived stem cells (ADSCs) were used to produce spheroids by the hanging-drop method. The spheroids were then loaded into a porous scaffold and induced to differentiate into cartilage. To confirm the cartilage phenotype of the differentiated spheroids in the scaffold, the complex was evaluated for the expression of chondrogenic-related genes and proteins. The cartilagenous tissues formed from the spheroid-scaffold complexes were primarily checked for *in vivo* functioning by transplanting them into rat models of cartilage damage. The results showed that the spheroid-scaffold complexes displayed the cartilage phenotype after inducing chondrogenic differentiation. The complexes stained positive with safranin O, alcian blue and collagen 2,

significantly expressed Sox9, Col2, and aggrecan genes compared with that before differentiation. *In vivo*, the differentiated spheroid-scaffold complexes formed mature cartilage that stained strongly positive with safranin O and fast red. These results suggest a promising strategy to produce cartilaginous microtissue for regenerative medicine.

2. INTRODUCTION

Cartilaginous lesions are often difficult to treat because cartilage has limited self-healing and self-regenerative abilities (1). Cartilage is an avascular connective tissue with a low metabolic rate and is formed by cartilage cells attached to small niches in the extracellular matrix (ECM) (2). The ECM encapsulates mature chondrocytes in the lacunae, which cannot proliferate (3). Thus, chondrocytes rarely exhibit cell-to-cell interaction. Chondrocytes have a very low replication rate, which is the main reason for the low regeneration of injured cartilage (4).

For decades, many strategies have been used to heal cartilage defects, including surgical techniques such as induced chemical therapies, cell therapies (5), scaffold-based solutions (6), and tissue engineering (7). Clinical studies have shown that articular cartilage recovered *via* traditional surgical methods normally expresses collagen 1 (Col1), which is typical of fibrocartilage. This differs from that expressed in nature (hyaline cartilage) (8). Compared with traditional surgical methods, tissue engineering has gradually shown superiority over other methods. Models created by tissue engineering greatly affect signaling pathways, thus stimulating recovery and/or repairing damaged tissues (9,10).

Several cell types have been examined for their capacity to repair injured cartilage. Mesenchymal stem cells (MSCs) derived from bone marrow (11,12), adipose tissue (13-15), umbilical cord, and synovium (16) can effectively treat cartilage. In addition, chondrocytes or chondroprogenitor cells are sources of cartilage regeneration (17,18). However, acquiring chondrocytes from humans is invasive, and finding a qualified source is difficult (19). Therefore, stem cells, especially those from easily acquired sources (such as adipose tissue) are popular in regenerative medicine and research applications. Compared with research studies on tissue repair and regeneration, applications that use cells and scaffolds show great potential for increasing cell seeding quantities on scaffolds (7). Many studies have used high cell densities during differentiation to create cartilaginous tissues to mimic natural chondrogenesis but that can also settle and form ECM more easily (20). With the growing popularity of 3D culture technology, many tissue regeneration strategies will rely on 3D-applied free-scaffolds or cell-scaffold models.

Various scaffolds are used to engineer cartilaginous tissue; the current study used VariotisTM. Variotis is a porous synthetic polymer scaffold that is highly spongey (> 95%) with a niche diameter of approximately 200 µm. VariotisTM is free of viruses, bacteria, proteins and exotic nucleic acids and is approved by the Food and Drug Administration (21). This material has been developed for use in cartilage repair therapies and is currently being used extensively in treatment of acute lesions as well as cancer research.

This study was conducted to produce *in vitro* cartilage tissue by differentiating spheroids of adipose-derived stem cells (ADSCs) on porous scaffolds under chondrogenesis differentiation conditions.

3. MATERIALS AND METHODS

3.1. Characterization of ADSCs

Human ADSCs were prepared and cryopreserved in a previous study at the Stem Cell Institute, University of Science, VNU-HCM, Viet Nam. The cryopreserved ADSCs were thawed and expanded to obtain enough cells for characterization and experimentation according to standard conditions and assays published in previous studies. ADSCs were examined for surface antigen expression using CD14-FITC, CD34-FITC, CD44-PE, CD45-APC, CD73-PerCP, CD90-PE, CD105-FITC, and HLADR-FITC (in a

Becton Dickinson FACSCalibur flow cytometry system). Briefly, the cell suspension was stained with monoclonal antibody conjugated with a fluorescent dye in the dark for 30 min. The cell suspensions were then washed twice to remove the extra monoclonal antibodies. Finally, cells were resuspended in fluid sheath buffer and analyzed for expression of the respective markers at 10000 cell events using CELLQuestPro acquisition software (BD Bioscience, Franklin Lakes, NJ, United States).

For *in vitro* differentiation, ADSCs were seeded at 5000 cells per well in a 96-well plate to confirm their differentiation potential. When cells adhered to the culture surface, chondrogenic (StemPro® Chondrogenesis Differentiation Media), osteogenic- (StemPro® Osteogenesis Differentiation Media), or adipogenic-induction medium (StemPro® Adipogenesis Differentiation Media) (Gibco/ThermoFisher Scientific, United States) was added individually to each well. The media were refreshed every 4 d. After 4 wk, the cells were fixed in 4% paraformaldehyde (Sigma-Aldrich, St. Louis, MO, United States). Chondrogenic, osteogenic, and adipogenic differentiated cells were stained with alcian blue, alizarin red, or oil red solution, respectively.

3.2. Spheroid culture

ADSCs were seeded at 1000 cells per cm2 in a T-75 flask with ADSCCult I medium (Regenmedlab, HCMC, Viet Nam). When the cells reached 80% confluency, ADSCs were passaged using deattachment solution (Regendmedlab, HCMC, Viet Nam). ADSCs from passages 5 to 10 were seeded onto a hanging-drop plate at 2000 cells, 4000 cells, 8000 cells or 10000 cells per well. Spheroid formation was observed microscopically on days 2, 4 and 6. The medium was refreshed every 3 days.

3.3. ADSC spheroid histology

Spheroids were harvested from the hanging-drop plate on days 3 and 7 and fixed in 4% paraformaldehyde. The spheroids were then embedded in paraffin and sectioned on slides at a thickness of 5–10 µm. The slides were stained with hematoxylin and eosin (HE) following standard protocol.

3.4. Controlling the cell survival/cell death ratio in the spheroids

Cells were washed with PBS and fixed in 4% paraformaldehyde for 30 min at room temperature (RT). Hoechst 33342 solution was used at 5 µL per 20 spheroids (10^5 cells) per 1 mL PBS and stained for 5 min at RT in the dark. The stained samples were centrifuged at 1000 rpm for 5 min at 4°C to remove the staining solution. Next, the spheroids were stained with 2 µLpropidium iodide (PI) at 20 spheroids per 1 mL PBS for 5 min in the dark. Finally, the spheroid cores were observed under a fluorescence microscope (Carl Zeiss, Germany).

3.5. Loading ADSC spheroids onto the porous scaffolds

Scaffolds were soaked in the culture medium for at least 30 min before being used in the experiments. A solution containing 192 spheroids was loaded onto the porous scaffold, then the scaffold in the solution was centrifuged at 200 × g for 2 min to push the spheroids inside the porous scaffold. The scaffold-spheroid complexes were incubated in culture medium at 37°C and 5% CO_2. After 2 h, 2 mL of ADSCCult I was added. The medium was refreshed every 3 days.

3.6. Chondrogenic induction of spheroid-scaffold complexes

To induce chondrogenic differentiation, the spheroid-scaffold complexes were cultured in chondrogenic induction medium (Thermo Fisher Scientific, Waltham, MA, United States), following a procedure similar to that of the *in vitro* chondrogenic ADSC differentiation. The differentiated medium was refreshed every 3 d for 30 d. This assay included 2 groups: Group 1 (G1) consisted of spheroid-scaffold complexes induced to differentiate into cartilage, while Group 2 (G2) consisted of uninduced spheroid-scaffold complexes (control group).

Table 1. Primer sequences used for reverse-transcription polymerase chain reaction

Gene Name	Forward primer	Reverse primer	Size of amplified product (basepair)	GenBank No	References
Sox9	AGG ACC CGG ATT ACA AG	CCT TGA AGA TGG CGT TGG G	117	NM_000346.3	(23)
Col2a1	ATC CGG TAT TAG GGT CGC TTG	GAG CGA CTG GAA GGT TT	115	XM_017018831.1	(23)
Aggrecan	TCGAGGACAGCGAGGCC	TCGAGGGTGTAGCGTGTAGAGA	85	XM_017021987.1	(23)
β-actin	AGAGCTACGAGCTGCCTGAC	AGCACTGTGTTGGCGTACAG	184	NM_001101.4	(24)
RUNX2	GGAGTGGACGAGGCAAGAGTTT	AGCTTCTGTCTGTGCCTTCTGG	133	XM_011514966.2	(23)
ChM1	GCGCAAGTGAAGGCTCGTAT	GTTTGGAGGAGATGCTCTGTTTG	64	XM_011534898.2	(25)
Col1a1	TGACTGGAAGAGCGGAGAGT	TCTCTCCAAACCAGACGTGC	185	XM_005257059.4	(26)

3.7. Histological analysis

Spheroid-scaffolds complexes in G1 and G2 were collected after 30 d of culturing, fixed in 4% paraformaldehyde, embedded in paraffin, and sectioned into 5–10 µm slices. The slices were stained with safranin O and alcian blue following the protocol of Tas *et al* (22). Histological sections were examined under light microscopy.

3.8. Immunohistochemical staining

Immunohistochemical staining was performed for collagen type II (Col2). After deparaffinization, sections were soaked in Tris-EDTA at pH 9.0 at 100°C for 20 min, then blocked with 10% goat serum/ Tris-buffered saline (TBS) (Invitrogen) for 1 h at RT. These sections were stained with Col2 primary antibody (M2139; Thermo Fisher Scientific) at 1:10 in 1% bovine serum albumin (BSA) /TBS at 4°C overnight. Sections were then washed with TBST (TBS with 0.1% Triton × 100) 3 times for 10 min each before staining with secondary antibody (mouse-IgG kappa (sc-516141, Santa Cruz, Santa Cruz, CA, United States) at 1:50 in 1% BSA/TBS for 60 min at RT in the dark. The unbound secondary antibodies were then washed off with TBST (at least 5 times for 10 min). Cellular nuclei were counterstained with mounting medium containing DAPI at RT. Sections were examined under confocal microscopy (LSM 750; Carl Zeiss).

3.9. RNA extraction and gene expression analysis

RNA was isolated from the spheroid-scaffold complexes of both G1 and G2 on days 15 and 30 using the Easy Spin RNA Total Extraction kit (Intron, Korea) per the manufacturer's instructions. One-step quantitative RT-PCR was performed for 7 genes: Sox9, Collagen 1a1, Collagen 2a1, Aggrecan, ChM1, Runx2, and beta-actin (reference gene). The reaction conditions used were those listed in the qPCRBIO Sygreen 1-Step Detect Lo-ROX Kit manual (PCRBioSystems, United Kingdom). Primer sequences used for reverse-transcription polymerase chain reaction (Table 1) (23-26).

3.10. *In vivo* functions of cartilage tissues formed from spheroid-scaffold complexes

To confirm the *in vivo* function of the cartilage formed from the spheroid-scaffold complexes, the cartilage was transplanted into immunosuppressed female rat models of cartilage damage at the hindlimb knee. Immunosuppression was induced in the rats by injecting a combination of busulfan and cyclophosphamide, then the injury was produced in the rat models by subchondral drilling of the hind limb knee using a drill with a 2 mm diameter needle after the skin was opened at the joint. Rats were anesthetized during the procedure. The institutional ethical committee about animal usage and care approved all

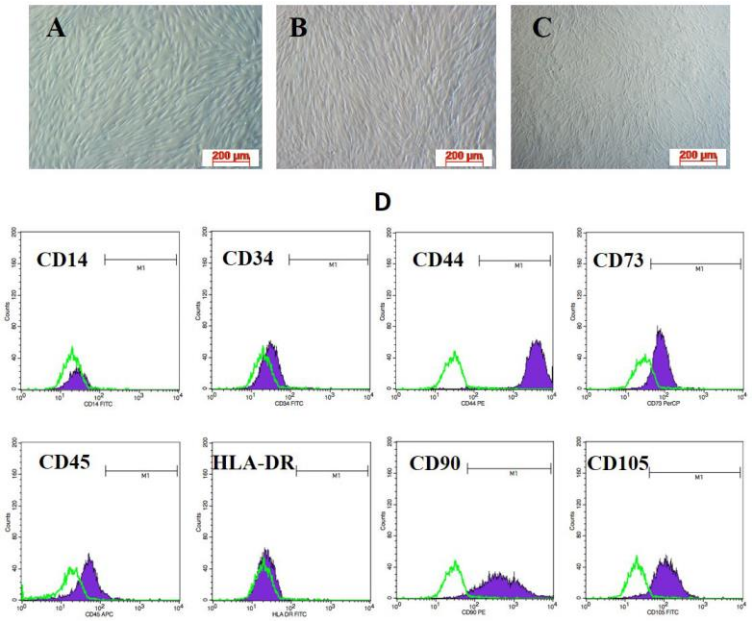

Figure 1. Shape and immunophenotype of human adipose-derived stem cells after thawing and subculture to passage 10. A: The shape of human adipose-derived stem cells at passage 2; B: At passage 5; C: At passage 10; D: These cells expressed mesenchymal stem cell specific markers, including CD44, CD73, CD90 and CD105, but were negative for CD14, CD34, CD45 and HLADR. CD: Cluster of differentiation; HLA: Human leukocyte antigen. (A-C: 10 × Magnification). Scale bar (A-C): 200 μm

procedures (No. 10 Laboratory of Animal Usage and Care /SCI).

After drilling, the cartilage was placed in the hole, then the skin was closed, and the wound was treated and monitored for 12 wk. The animals were maintained at the Laboratory of Animal Usage and Care in isolated cage at 21 ± 2°C and 60 ± 5% relative humidity with full ventilation under a 12 h light/dark cycle (7 a.m.-7 p.m.), and they had access to food and water ad libitum.

After 12 wk, the rats were killed, and the joints were collected to evaluate the phenotype of the cartilage at the transplantation sites using safranin O-fast red staining. Five female rats were used in this experiment.

4. RESULTS

4.1. Characterization of ADSCs

In the 2D culture, ADSCs adhered and spread on the culture surface and displayed an elongated shape (similar to fibroblasts). This state was maintained after passages 2 (Figure 1A), 5 (Figure 1B), and 10 (Figure 1C) without a significant change in shape. Flow cytometry analysis demonstrated a homogenous MSC population (Figure 1). The ADSCs stained positive for CD44 (98.03%), CD73 (93.05%), CD90 (97.58%), CD105 (95.52%), and were negative for CD14 (0.14%), CD34 (0.51%), CD45 (2.4%), and HLADR (0.24%).

Under adipogenesis induction, ADSCs accumulated as lipid droplets inside the cytoplasm, which was detected from day 8 postinduction. These lipid droplets gradually increased in size and were clearly visible under an inverted microscope on day 15. To verify the lipid droplets, we stained the cells with oil red dye, and the lipid droplets stained red (Figure 2A). After inducing chondrogenesis, the ADSCs changed their shape from day 7 on, expressing and accumulating more ECM. After 21 d of induction, the cells were stained with alcian blue dye to detect glycosaminoglycans, and the cells stained positive (Figure 2B). Under the osteogenic condition, the ADSCs also changed their shape from

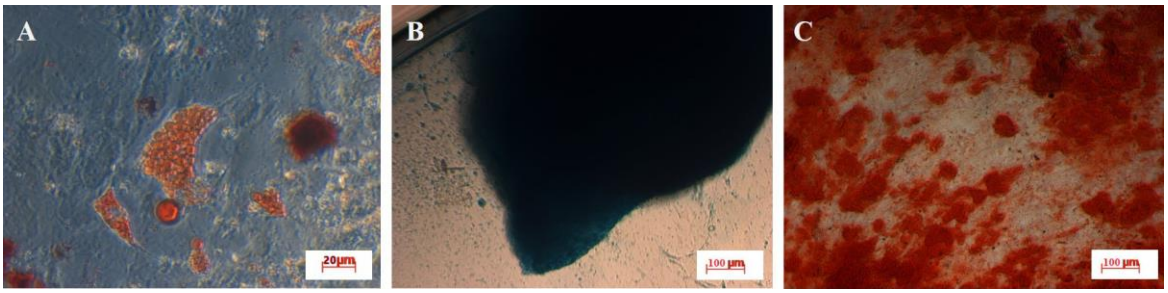

Figure 2. *In vitro* differentiation potential of human adipose-derived stem cells into mesoderm cell lineage. A: Human adipose-derived stem cells could be differentiated into adipocytes; B: Human adipose-derived stem cells could be differentiated into chondrocytes; C: Human adipose-derived stem cells could be differentiated into osteoblasts. (A: 20 × Magnification; B, C: 5 × Magnification). Scale bar: 20 µm (A), 100 µm (B-C)

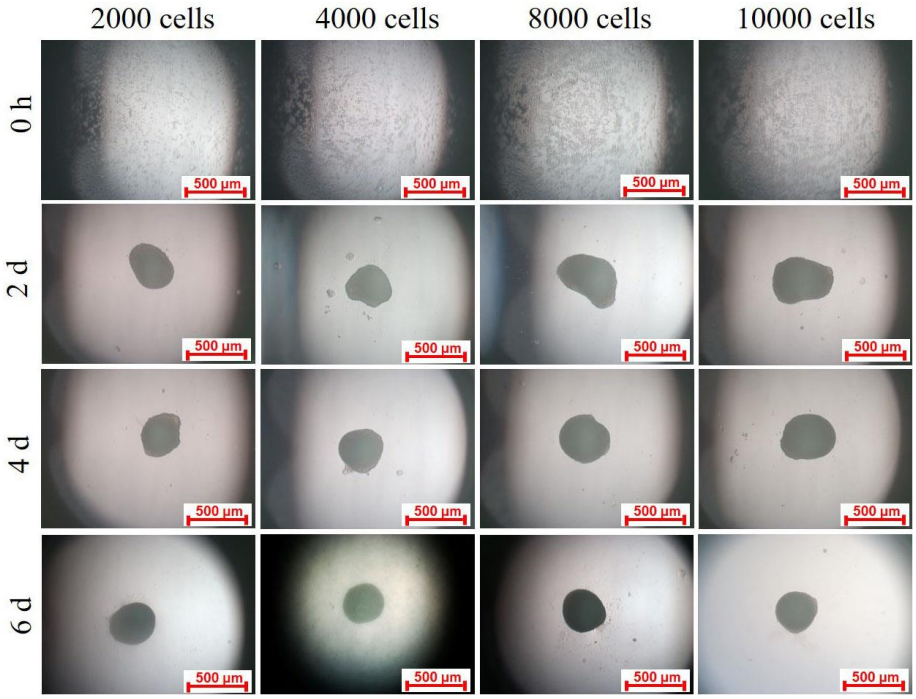

Figure 3. The adipose-derived stem cell spheroids formed under various different concentrations of adipose-derived stem cells using the hanging drop condition. (5 × Magnification). Scale bar: 500 µm

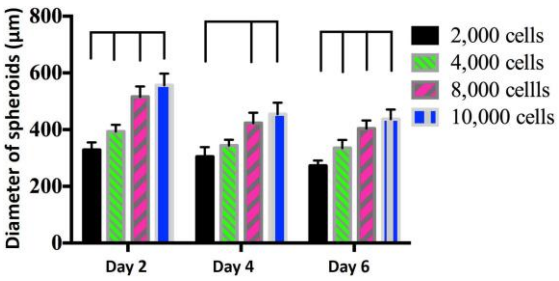

Figure 4. The spheroid size at different cell densities at days 2, 4 and 6. The spheroids of 4000 cells were more stable than those in the other groups. $P < 0.05$: Statistically significant.

day 7 onward, accumulating ECM with high concentrations of Ca^{2+} and Mg^{2+} that stained positive with alizarin red (Figure 2C).

4.2. Production of ADSC spheroids

Cells were cultured in a hanging-drop plate at different densities. At $t = 0$, cells initially existed individually (Figure 3) suspended inside the hanging drop. These cells were pulled together by gravity to form spheroids after several days of culturing. Optical

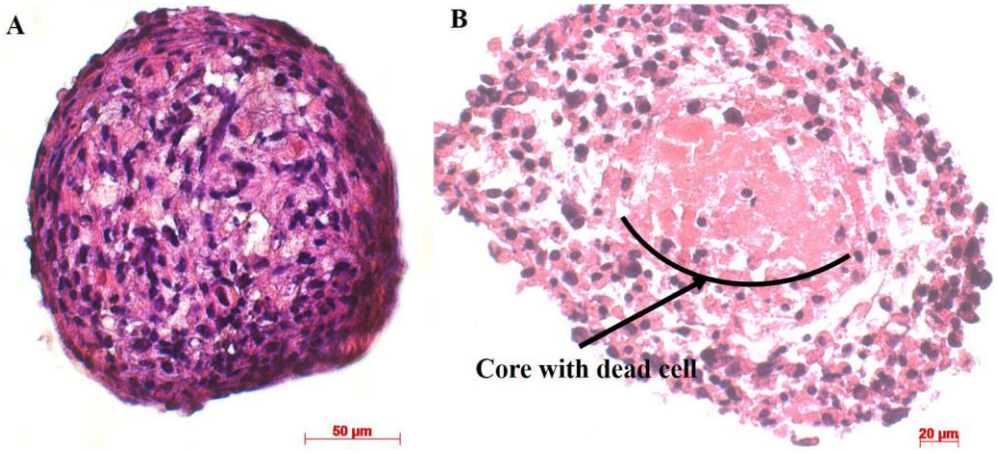

Figure 5. The slides of adipose-derived stem cell spheroids were stained with hematoxylin eosin to display the structure of the spheroids. The adipose-derived stem cell spheroids displayed the cores with dead cell as a particular structure of spheroids. (A, B: 20 × Magnification).

microscopy showed that the spheroids formed at an early stage (after 1–2 d), often had thin borders, and were easier to see than those in the later stages, where the cells had already interacted with other cells to form more tightly bound solids.

After 2 d of incubation under handing-drop conditions, the ADSC spheroid sizes differed significantly between cell densities. Higher cell concentrations produced larger ADSC spheroids (328.5 ± 26.35 µm at 2000 cells; 393.2 ± 23.88 µm at 4000 cells; 515.43 ± 36.90 µm at 8000 cells; and 556.0 ± 41.94 µm at 10000 cells; $P < 0.05$; Figure 3). After 4 d of culturing, the diameters did not differ (304.3 ± 34.12 µm at 2000 cells; 343.4 ± 21.0 µm at 4000 cells; 423.25 ± 36.28 µm at 8000 cells; and 454.05 ± 40.72 µm at 10000 cells). However, on day 6, the spheroid diameters differed again: 272.51 ± 18.36 µm at 2000 cells; 335.08 ± 28.72 µm at 4000 cells; 403.87 ± 28.43 µm at 8000 cells; and 436.94 ± 33.97 µm at 10000 cells.

Spheroids at the same cell densities gradually decreased in size from day 2 to days 4 and 6. At spheroids of 2000 cells, the spheroid diameter decreased from 328.5 ± 26.35 µm to 304.3 ± 34.12 µm to 272.51 ± 18.36 µm on days 2, 4 and 6, respectively. The reduction in size from day 2 to day 4 was nonsignificant, but that from day 4 to day 6 was significant ($P < 0.05$) (Figure 4). However, at the higher cell densities (4000; 8000 and 10000 cells), the diameters decreased at faster rates. Compared with those on day 2, the spheroid diameters on day 4 were significantly reduced in both groups ($P < 0.05$; 393.2 ± 23.88 µm on day 2 *vs* 343.4 ± 21.0 µm on day 4 for spheroids of 4000 cells; 515.43 ± 36.90 µm on day 2 *vs* 423.25 ± 36.28 µm on day 4 for spheroids of 8000 cells; and 556.0 ± 41.94 µm on day 2 *vs* 454.05 ± 40.72 µm on day 4 for spheroids for 10000 cells). However, these sizes decreased nonsignificantly from days 4 to 6 ($P > 0.05$; 343.4 ± 21.0 µm on day 4 *vs* 335.08 ± 28.72 µm on day 6 for spheroids of 4000 cells; 423.25 ± 36.28 µm on day 4 *vs* 403.87 ± 28.43 µm on day 6 of spheroids of 8000 cells; and 454.05 ± 40.72 µm on day 4 *vs* 436.94 ± 33.97 µm on day 6 for spheroids of 10000 cells) (Figure 4).

Hence, the different initial densities for the 3D cell block formation were based on the size reduction over time until the cell block reached a stable structural state. The suitable densities selected for the next experiments on the porous scaffolds were 2000 and 4000 cells. For the stability criteria of size over time, the 4000-cell density was preferred since the spheroid size stabilized from day 4 onward.

The HE-stained slides show the ADSC spheroid structure with a dead cell in the center (Figure 5). The high cell densities were mainly

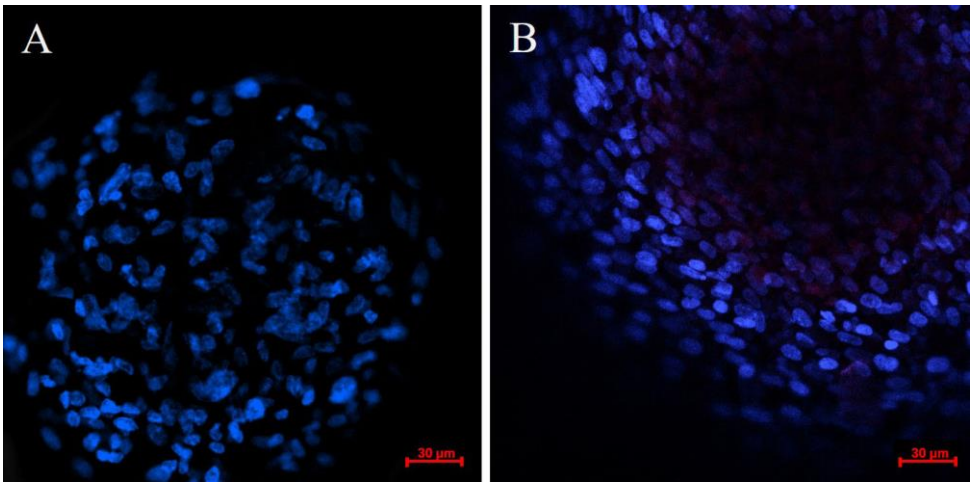

Figure 6. The core with dead cell was stained with propidium iodide and Hoechst 33342. A: Spheroids which had not formed cores with dead cell; B: Those which formed cores with dead cell. The pictures were captured under confocal microscopy. (A, B: 20 × Magnification). Scale bar: 30 µm

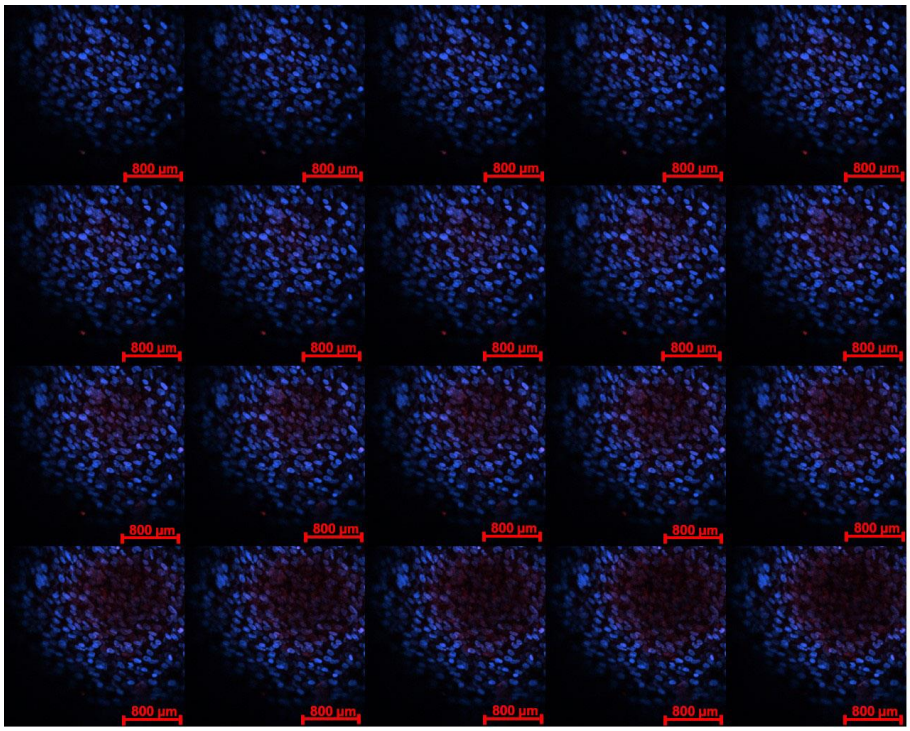

Figure 7. The appearance of a core with dead cell in the spheroids was captured by confocal microscope by staining with propidium iodide and Hoechst 33342. The dead cells were positive with propidium iodide stain and had the defragmented nuclei situated at the center of spheroids. (20 × Magnification). Scale bar: 800 µm

concentrated in the outer membrane of the spheroids, and the cell density gradually decreased to the inner membrane. To confirm the cores with dead cells in the spheroid center, the spheroid slides were stained with Hoechst 33342 and PI (Figure 6). The early stage (day 3) contained no dead cells in the spheroid (Figure 6A). However, when cells in this spheroid interacted more tightly, dead cells appeared

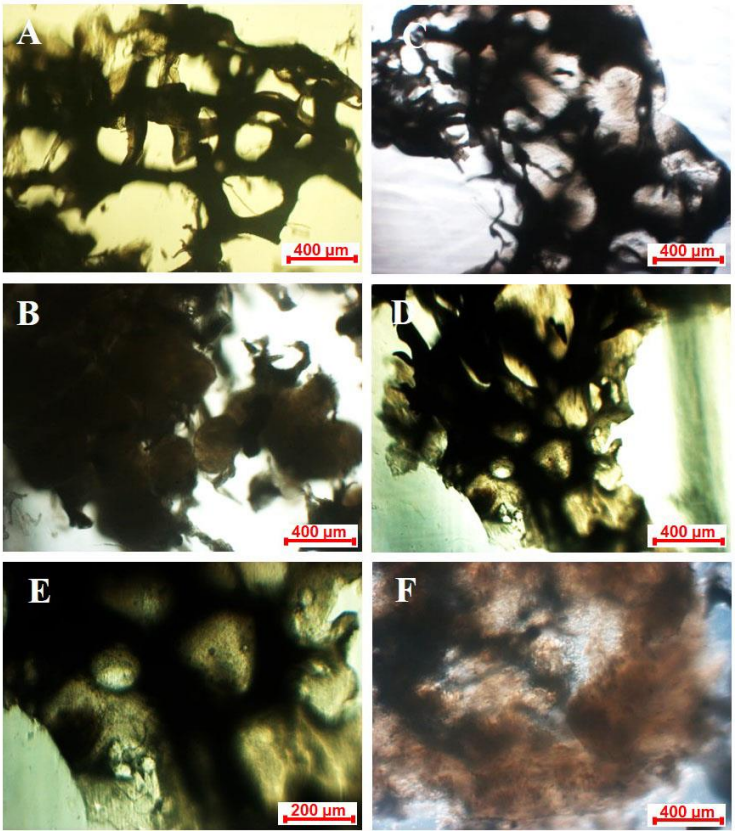

Figure 8. The adipose-derived stem cell spheroids loaded onto porous scaffolds were capable of adhering and growing. A: Porous scaffold; B: 0 h; C: 4 d; C: 7 d; D: 15 d; E: Before induced differentiation; F: After induced differentiation. (A, B, C, D, F: 5 × Magnification; E: 10 × Magnification). Scale bar: 400 μm (A, B, C, D, F), 200 μm (E)

that stained positive with PI (Figure 6B). The existence of the dead-cell core in the 3D spheroid was more clearly visible *via* confocal microscopy (Figure 7).

4.3. ADSC spheroid growth and differentiation on scaffolds to cartilage

After ADSC spheroids were loaded onto scaffolds, cells in the outer membrane of the spheroids could adhere onto the scaffold surface and were expanded. Therefore, the spheroids nearly filled all porous scaffolds after 15 d (Figure 8B–D). At day 15, the ADSC spheroid and scaffold complexes were induced to differentiate into cartilage in the inducing media, similar to that of the 2D differentiation.

The existence and growth of the ADSC spheroids on the porous scaffolds were also evaluated using scanning electron microscopy (Figure 9). The porous scaffold had a rough surface with different pore sizes (Figure 9A). The ADSC spheroids were attached on the scaffold surfaces (Figure 9B). After induction into cartilage, the scaffold surface was more compact with tiny pores (Figure 9C).

The induced cartilage structures (spheroid and porous scaffold complexes) were stained with HE (Figure 10) to view the structure of the complexes and cartilage-like complexes. After 15 d of induction, the structure of the induced complexes differed from that of the uninduced controls; the ADSCs were restructured and rearranged in the induced complexes. Under inducing conditions, the ADSCs secreted more ECM, and the link between cells was more condensed.

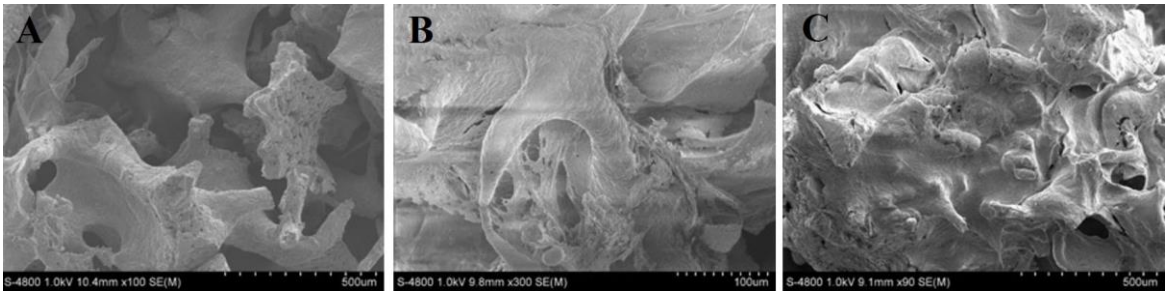

Figure 9. Scanning electron microscope captures of scaffold and complexes of scaffold and spheroids. A: The porous structure of scaffold; B: The adipose-derived stem cell spheroids adhering on the surface of scaffold; C: The compact structure of complexes of adipose-derived stem cell spheroids and scaffold after induction into cartilage. (A: 100 × Magnification; B: 300 × Magnification; C: 90 × Magnification). Scale bar: 500 μm (A, C), 100 μm (B)

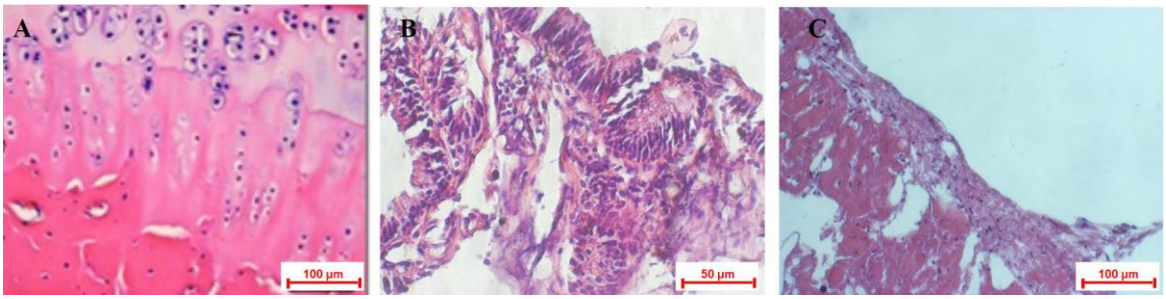

Figure 10. The structure of induced cartilage (induced complexes of spheroids and scaffold) compared to un-induced complexes of spheroids and scaffold, as well as the natural human cartilage. A: The slide of nature human cartilage Musumeci *et al* (50); B: Un-induced complexes of spheroids and scaffold; C: Induced complexes of spheroids and scaffold. (A: 20 × Magnification; B, C: 10 × Magnification). Scale bar: 100 μm (A,C), 50 μm (B)

To verify that the induced spheroid and scaffold complexes were indeed cartilage, the slides from the induced spheroid and scaffold complexes were stained with alcian blue and safranin O (Figure 11). Unlike the uninduced complexes, all induced complexes showed strong positive staining with both safranin O (red) and alcian blue (Figure 11).

Immunohistochemical analysis of cartilage-specific proteins (*e.g.*, collagen type II) was performed to confirm the induced spheroid and scaffold complexes exhibiting cartilaginous properties. The induced complexes were strongly positive for collagen type II compared with that of the control group (uninduced complexes; Figure 12). However, in the uninduced condition, the complexes also expressed collagen type II at low levels (Figure 13). To compare the expression levels of collagen type II between the induced and uninduced complexes, the immunohistochemical images were uploaded to Image J software to identify the collagen type II-positive areas. The results showed that 20.07 ± 3.57% of the slide area in the control group was positive, while 60.74 ± 2.74% of the slide area in the induced group was positive ($P < 0.0001$; Figure 13).

Finally, the induced cartilage was confirmed by chondrocyte-specific gene expression, including sox9, collagen2, aggrecan, and chondromodulin 1. Col1 and Runx2 did not did significantly differ from the control groups (uninduced) compared with the induced complexes after 15 and 30 d of induction (Figure 14). However, after 30 d, the expressions of these genes were significantly decreased ($P < 0.001$) compared with those at day 15 and were nonsignificantly higher than those of uninduced complexes.

4.4. The induced spheroid-scaffold complexes displayed the mature cartilage phenotype *in vivo*

After 12 wk, five rats were healthy, without any advese effects observed. The joints from five rats

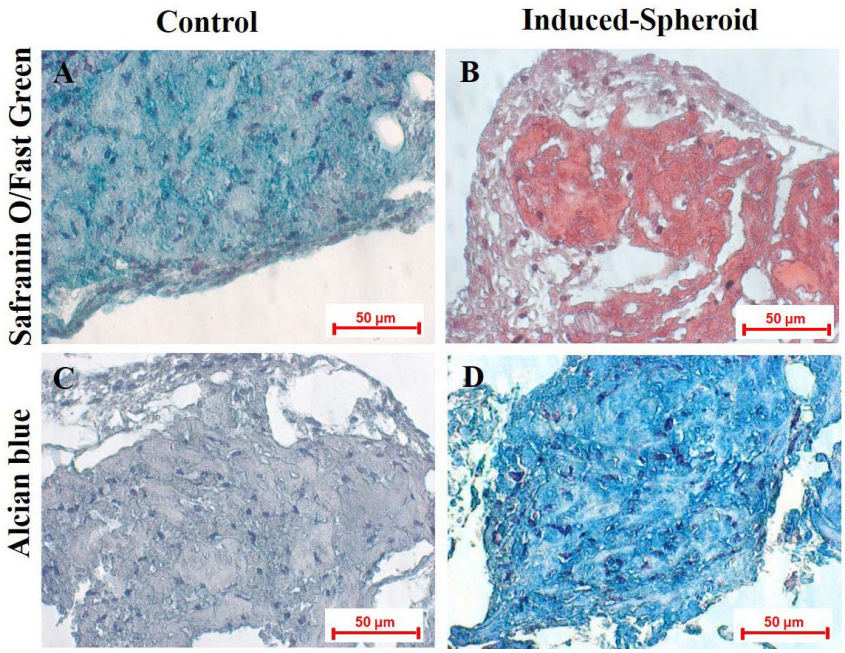

Figure 11. The induced complexes of spheroids and scaffold stained positive with Safranin O and Alcian blue dye, compared to un-induced complexes. A: while the un-induced complexes were negative with Safranin O; B: The induced complexes were positive with Safranin O; C: while the un-induced complexes were negative with Alcian blue; D: The induced complexes were positive with Alcian blue. (A-D: 5 × Magnification). Scale bar: 50 µm (A,B,C,D)

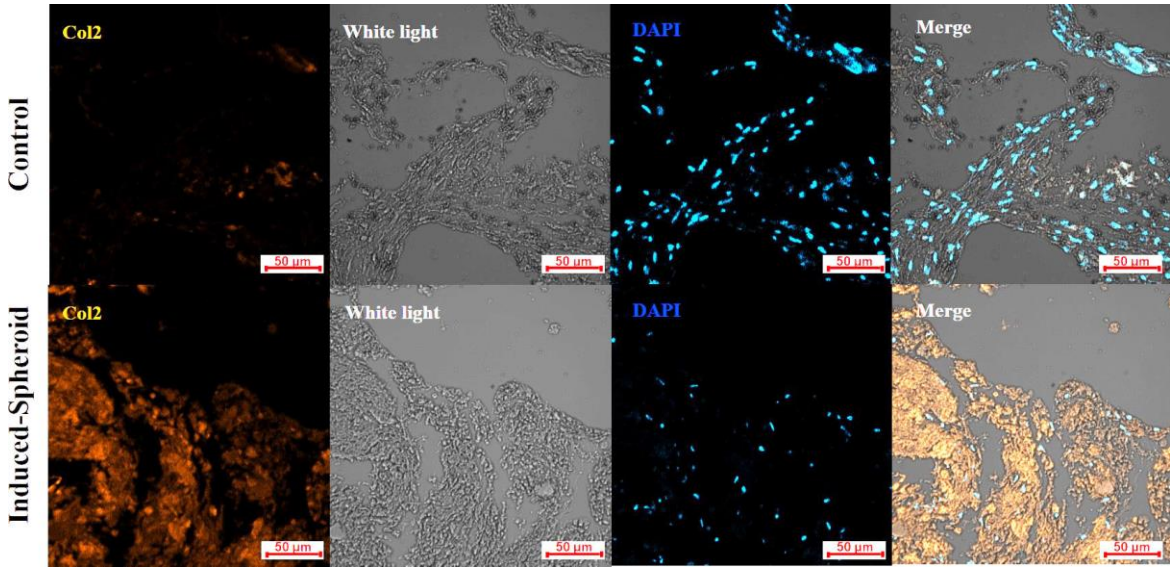

Figure 12. The expression of collagen 2 in induced complexes of spheroids and scaffold compared to un-induced complexes of spheroids and scaffold. Collagen 2 was significantly expressed in the induced complexes of spheroids and scaffold compared to un-induced ones. (20 × Magnification). Scale bar: 50 µm

with complexes of induced spheroid-scaffold were collected to evaluate the phenotype of cartilage; and the normal joints (without transplantation of induced spheroid-scaffold

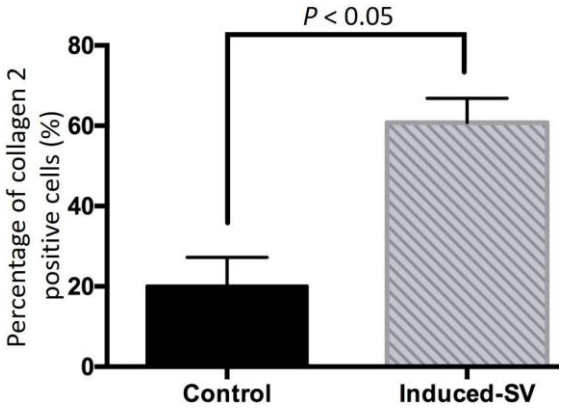

Figure 13. The expression level of collagen type 2 in the induced and un-induced complexes of spheroids and scaffold. In the induced complexes, collagen type 2 showed a significantly higher expression than in un-induced complexes. P < 0.05: Statistically significant.

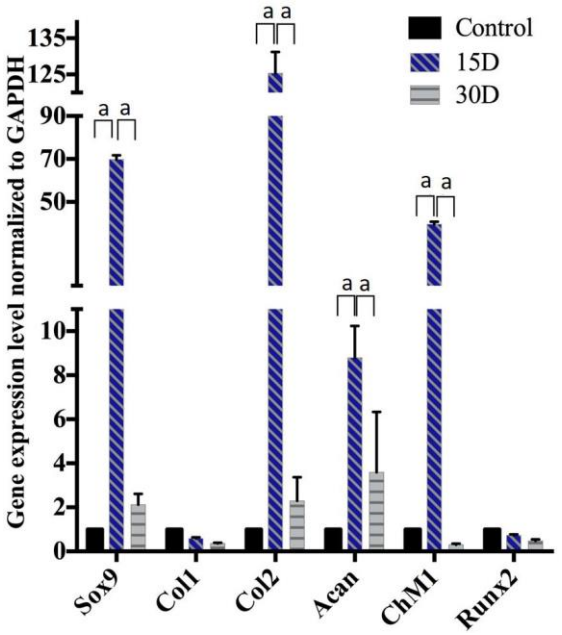

Figure 14. The cartilage-specific gene expression level. The gene expression of Sox9, Collagen 1, Collagen 2, Aggrecan, Chondromodulin 1, and Runx2 of complexes of adipose-derived stem cell spheroids and scaffold were compared at day 15 and day 30 after induction, to un-induced group (control). Col1: Collagen 1; Col2: Collagen 2; Acan: Aggrecan; ChM1: Chondromodulin 1; a: P < 0.05 (statistically significant).

complexes) also were collected and used as control.

The cartilage at the transplanted sites stained strongly positive (red) with safranin O-fast red (Figure 15). The results confirmed that the spheroid-scaffold complexes that were induced to cartilage *in vitro* could become mature cartilage *in vivo*, similar to natural cartilage.

5. DISCUSSION

Combining spheroids and scaffolds is a cutting-edge approach in tissue engineering. Compared with single-cell seeding on scaffolds, spheroids exhibit many advantages. Many researchers have implanted spheroids on 3D scaffolds to transplant these models to repair bone or cartilage damage in animals (1,27,28). Therefore, in this study, we aimed to produce cartilage *in vitro* by combining ADSC spheroids on a porous scaffold.

We first produced the ADSC spheroids. Formation of spheroids at different cell densities yielded different spheroid sizes. After culturing, the spheroids formed cores with dead cells. In the early days of formation, interactions between cells were relatively loose, but after a few days, when the cell interactions became tighter, necrosis occurred at the spheroid core due to lack of oxygen distribution and nutrients for proliferation (29,30). At this time, the spheroid sizes stabilized and were normally smaller than at the early stage when cell aggregation was just forming. Spheroid sizes increased slightly in the following days, followed by an increase in the dead-cell area.

Cancer cells usually take 7–14 d to form a stable spheroid (31-33). In our study, ADSCs took less than 7–14 d to form spheroids owing to the presence of specific adhesion markers, such as N-cadherin and CD90, and the homogeneous ADSC surface (34).

In the next step, ADSC spheroids were loaded onto the porous scaffold to produce the spheroid and scaffold complexes. After 15 d of loading, ADSC spheroids adhered and grew on the scaffold to fill the scaffold pores. Compared with single ADSC loading onto the porous scaffold, cells took 3–8 wk to fill the scaffold (15,35). Thus, spheroid loading can reduce the

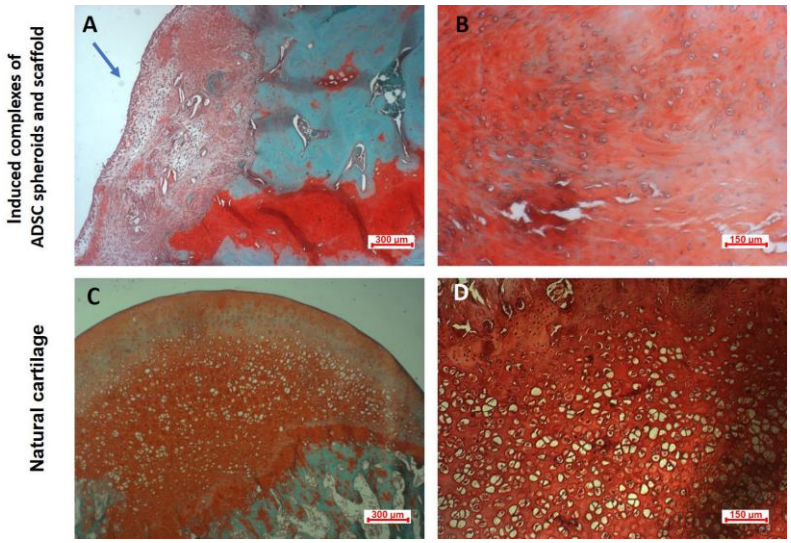

Figure 15. Induced complexes of adipose-derived stem cells spheroids and scaffold toward cartilage exhibited the normal structure of cartilage. A, B: Induced cartilage were strongly positive with Safranin O–Fast Red staining, similar to the natural cartilage; C, D: Natural cartilage . Arrow (in the Figure A): Site of induced complexes of adipose-derived stem cells spheroids and scaffold. ADSC: Adipose-derived stem cells. (A,B: 5 × Magnification; B,D: 10 × Magnification). Scale bar: 150 µm (A,C); 300 µm (B,D)

time to fill the scaffold compared with that of single-cell loading.

After 15 d of loading, the ADSC spheroid and scaffold complexes were induced in specific media to differentiate into cartilage. After 15 d of induction, the ADSC spheroid-scaffold complexes exhibited cartilage-specific properties and induced cartilage *in vitro*. The induced cartilage was characterized as *in vivo* cartilage by evaluation at the molecular, protein and histological levels.

The gene expressions of Sox9, Col2 and aggrecan (Acan) increased markedly after induction to cartilage. Wright (1995) proposed that cartilage production was related to Sox9 (36). The Sox9 transcriptional factor has been shown to be necessary in promoting mesenchymal cell entry into the cartilage differentiation program; thus, if Sox9 is absent, the process of creating cartilage will be blocked (37). Sox9 directly activates cartilage differentiation markers (38) and induces Sox5 and Sox6 expressions together with the cartilage differentiation program (39). Sox9 has been shown to be an important regulatory factor affecting cartilage-cell phenotypes and controls the expression of genes encoding cartilage substrate proteins, such as Col2a1 (38,40), Col9a1 (41), Col11a2 (42), Acan (43) and connective cartilage protein. Zhao *et al* (44) found that Sox9 and Col2a1 were coexpressed in all precursor cartilage cells, which is consistent with the observation that cartilage cells have elevated expression levels of Sox9 and Col2a. However, when cartilage grows and matures into the enlarged cartilage phase, only low levels of Col2a1 RNA are detected, which are almost without Sox9 expression (45). This may explain the reduced Sox9 and Col2 expressions after 30 d of induction, with no statistically significant differences compared with the control group.

ChM1 is a protein that inhibits angiogenesis in cartilage (46). ChM1 was expressed clearly in the primary cartilage, and the expression gradually decreased as the cartilage matured to prepare for hypertrophy (47). Col1 is expressed in mesenchymal cells from condensation to start the chondrogenesis process. However, when mesenchymal cells transformed to chondroprogenitors or chondroblasts, Col1 simultaneously transformed to Col2 (48). In addition, Runx2 is a marker of hypertrophic cartilage (49). In this study, Runx2 expression was low, demonstrating that induced spheroids were still

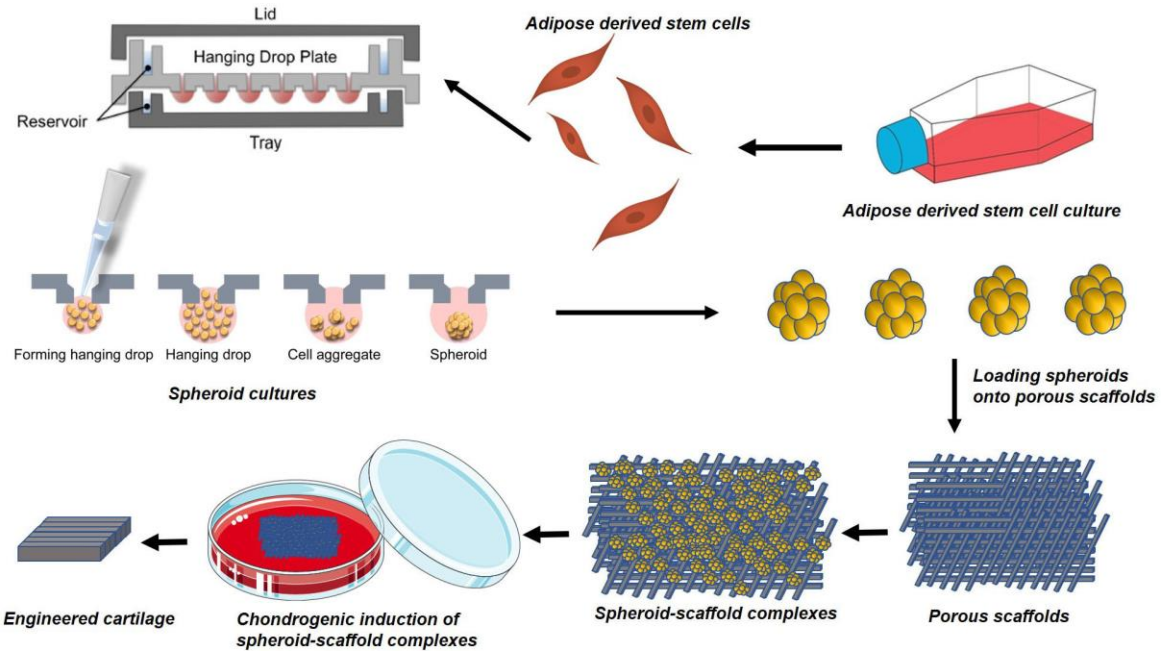

Figure 16. Engineered cartilage can be produced by *in vitro* cartilage differentiation of human adipose-derived mesenchymal stem cell spheroids cultured in porous scaffolds. In the first step, human adipose-derived mesenchymal stem cells were expanded *in vitro* to get enough cells for spheroid culture in the next step. Then, these spheroids were loaded into the porous scaffolds before they were induced to cartilage in the chondrogenic medium.

produced in the mature cartilage phase but had not yet entered the hypertrophic cartilage phase.

Induced cartilage tissue also strongly expressed collagen type II, as detected by immunohistochemistry. More importantly, the cartilage structure was confirmed when the slides of the induced cartilage stained positive with safranin O and alcian blue. These results confirmed that the induced ADSC spheroid-scaffold complexes displayed some cartilage-specific properties.

In the last experiment, we confirmed that the spheroid-scaffold complexes induced toward cartilage became mature cartilage after transplantation into rat models of cartilage damage. The color of the safranin O and fast red stains showed that the induced cartilage from the spheroid-scaffold complexes was similar to that of natural cartilage. The results primarily showed that the spheroid-scaffold complexes induced toward cartilage exhibited the cartilage phenotype both *in vitro* and *in vivo*.

This study demonstrated that ADSC spheroids loaded onto porous scaffolds can produce cartilage *in vitro* (Figure 16). The *in vitro* cartilage exhibited some properties of *in vivo* cartilage, including positive safranin O and alcian blue staining, significantly increased collagen II expression, and upregulated Sox9, Collagen2, and Acan genes after 15 and 30 d of induction to cartilage. These cartilaginous tissues also displayed the normal structure with the cartilage phenotype *in vivo*. These results suggest a new method for producing cartilage microtissue for regenerative medicine.

6. ACKNOWLEDGMENTS

This work is supported by Vietnam National University Ho Chi Minh City, No. TX2018-18-02. Authors declare no conflict of interest. Pham PV and Vu NB suggested the idea, designed the experiments, revised the manuscript, isolated, expanded and analyzed the mesenchymal stem cells from adipose tissue, analyzed the data, and evaluated the spheroid structure via confocal microscopy. Le HTN created the spheroids from

adipose-derived stem cells, evaluated the spheroid adhesion on the scaffold, the spheroid-scaffold complex structure, and the differentiation of the spheroid-scaffold complex into cartilage, and wrote the results and discussion. Nguyen PDN prepared the figures, wrote the introduction, and evaluated the spheroid differentiation. Dao TTT performed the reverse-transcription polymerase chain reaction and histochemistry analysis. To XHV performed the immunohistochemistry. All authors read and approved the manuscript. ORCID number: Ha Thi -Ngan Le (0000-0001-8503-5138); Ngoc Bich Vu (0000-0003-4447-9212); Phuc Dang-Ngoc Nguyen (0000-0001-5972-5266); Thuy Thi -Thanh Dao (0000-0002-9460-5427); Xuan Hoang-Viet To (0000-0001-6206-733X); Phuc Van Pham (0000-0001-7254-0717).

7. REFERENCES

1. LS Baptista, GS Kronemberger, I Côrtes, LE Charelli, RAM Matsui, TN Palhares, J Sohier, AM Rossi, JM Granjeiro: Adult Stem Cells Spheroids to Optimize Cell Colonization in Scaffolds for Cartilage and Bone Tissue Engineering. Int J Mol Sci 2018, 19 (2018)
DOI: 10.3390/ijms19051285
PMid:29693604 PMCid:PMC5983745

2. AJ Sophia Fox, A Bedi, SA Rodeo: The basic science of articular cartilage: structure, composition, and function. Sports Health 1, 461-468 (2009)
DOI: 10.1177/1941738109350438
PMid:23015907 PMCid:PMC3445147

3. AR Phull, SH Eo, Q Abbas, M Ahmed, SJ Kim: Applications of Chondrocyte-Based Cartilage Engineering: An Overview. Biomed Res Int 2016, 1879837 (2016)
DOI: 10.1155/2016/1879837
PMid:27631002 PMCid:PMC5007317

4. Y Gao, S Liu, J Huang, W Guo, J Chen, L Zhang, B Zhao, J Peng, A Wang, Y Wang, W Xu, S Lu, M Yuan, Q Guo: The ECM-cell interaction of cartilage extracellular matrix on chondrocytes. Biomed Res Int 2014, 648459 (2014)
DOI: 10.1155/2014/648459
PMid:24959581 PMCid:PMC4052144

5. P Pastides, M Chimutengwende-Gordon, N Maffulli, W Khan: Stem cell therapy for human cartilage defects: a systematic review. Osteoarthritis Cartilage 21: 646-654 (2013)
DOI: 10.1016/j.joca.2013.02.008
PMid:23485933

6. K Futrega, JS Palmer, M Kinney, WB Lott, MD Ungrin, PW Zandstra, MR Doran: The microwell-mesh: A novel device and protocol for the high throughput manufacturing of cartilage microtissues. Biomaterials 62: 1-12 (2015)
DOI: 10.1016/j.biomaterials.2015.05.013
PMid:26010218

7. J Günter, P Wolint, A Bopp, Steiger J, Cambria E, SP Hoerstrup, MY Emmert: Microtissues in Cardiovascular Medicine: Regenerative Potential Based on a 3D Microenvironment. Stem Cells Int 2016: 9098523 (2016)
DOI: 10.1155/2016/9098523
PMid:27073399 PMCid:PMC4814701

8. C Chung, JA Burdick: Engineering cartilage tissue. Adv Drug Deliv Rev 60: 243-262 (2008)
DOI: 10.1016/j.addr.2007.08.027
PMid:17976858 PMCid:PMC2230638

9. R Cancedda, B Dozin, P Giannoni, R Quarto: Tissue engineering and cell therapy of cartilage and bone. Matrix Biol 22: 81-91 (2003)
DOI: 10.1016/S0945-053X(03)00012-X

10. MP Lutolf, JA Hubbell: Synthetic

biomaterials as instructive extracellular microenvironments for morphogenesis in tissue engineering. Nat Biotechnol 23: 47-55 (2005)
DOI: 10.1038/nbt1055
PMid:15637621

11. WJ Li, R Tuli, C Okafor, A Derfoul, KG Danielson, DJ Hall, RS Tuan: A three-dimensional nanofibrous scaffold for cartilage tissue engineering using human mesenchymal stem cells. Biomaterials 26: 599-609 (2005)
DOI: 10.1016/j.biomaterials.2004.03.005
PMid:15282138

12. RL Mauck, X Yuan, RS Tuan: Chondrogenic differentiation and functional maturation of bovine mesenchymal stem cells in long-term agarose culture. Osteoarthritis Cartilage 14: 179-189 (2006)
DOI: 10.1016/j.joca.2005.09.002
PMid:16257243

13. H Betre, SR Ong, F Guilak, A Chilkoti, B Fermor, LA Setton: Chondrocytic differentiation of human adipose-derived adult stem cells in elastin-like polypeptide. Biomaterials 27: 91-99 (2006)
DOI: 10.1016/j.biomaterials.2005.05.071
PMid:16023192

14. HA Awad, MQ Wickham, HA Leddy, JM Gimble, F Guilak: Chondrogenic differentiation of adipose-derived adult stem cells in agarose, alginate, and gelatin scaffolds. Biomaterials 25: 3211-3222 (2004)
DOI: 10.1016/j.biomaterials.2003.10.045
PMid:14980416

15. G Calabrese, R Giuffrida, S Forte, C Fabbi, E Figallo, L Salvatorelli, L Memeo, R Parenti, M Gulisano, R Gulino: Human adipose-derived mesenchymal stem cells seeded into a collagen-hydroxyapatite scaffold promote bone augmentation after implantation in the mouse. Sci Rep 7: 7110 (2017)
DOI: 10.1038/s41598-017-07672-0
PMid:28769083 PMCid:PMC5541101

16. A Yokoyama, I Sekiya, K Miyazaki, S Ichinose, Y Hata, T Muneta: *In vitro* cartilage formation of composites of synovium-derived mesenchymal stem cells with collagen gel. Cell Tissue Res 322: 289-298 (2005)
DOI: 10.1007/s00441-005-0010-6
PMid:16001268

17. SJ Bryant, KS Anseth: Hydrogel properties influence ECM production by chondrocytes photoencapsulated in poly (ethylene glycol) hydrogels. J Biomed Mater Res 59: 63-72 (2002)
DOI: 10.1002/jbm.1217
PMid:11745538

18. TJ Klein, BL Schumacher, TA Schmidt, KW Li, MS Voegtline, K Masuda, EJ Thonar, RL Sah: Tissue engineering of stratified articular cartilage from chondrocyte subpopulations. Osteo-arthritis Cartilage 11: 595-602 (2003)
DOI: 10.1016/S1063-4584(03)00090-6

19. R Seda Tigli, S Ghosh, MM Laha, NK Shevde, L Daheron, J Gimble, M Gümüşderelioglu, DL Kaplan: Comparative chondrogenesis of human cell sources in 3D scaffolds. J Tissue Eng Regen Med 3: 348-360 (2009)
DOI: 10.1002/term.169
PMid:19382119 PMCid:PMC2791320

20. L Freed, G Vunjak-Novakovic: Tissue engineering of cartilage. In: Bronzino JD. The biomedical engineering handbook. Boca Raton: CRC Press, Boca Raton,

2000: 124-126 (2000)
DOI: 10.1201/9781420049510.ch124

21. M Zhang, P Boughton, B Rose, CS Lee, AM Hong: The use of porous scaffold as a tumor model. Int J Biomater 2013: 396056 (2013)
DOI: 10.1155/2013/396056
PMid:24101930 PMCid:PMC3786466

22. J Tas: The Alcian blue and combined Alcian blue--Safranin O staining of glycosaminoglycans studied in a model system and in mast cells. Histochem J 9: 205-230 (1977)
DOI: 10.1007/BF01003632
PMid:65345

23. HH Lee, CC Chang, MJ Shieh, JP Wang, YT Chen, TH Young, SC Hung: Hypoxia enhances chondrogenesis and prevents terminal differentiation through PI3K/Akt/FoxO dependent anti-apoptotic effect. Sci Rep 3: 2683 (2013)
DOI: 10.1038/srep02683
PMid:24042188 PMCid:PMC3775095

24. D Baek, KM Lee, KW Park, JW Suh, SM Choi, KH Park, JW Lee, SH Kim: Inhibition of miR-449a Promotes Cartilage Regeneration and Prevents Progression of Osteoarthritis in *In vivo* Rat Models. Mol Ther Nucleic Acids 13: 322-333 (2018)
DOI: 10.1016/j.omtn.2018.09.015
PMid:30326428 PMCid:PMC6197768

25. M You, G Peng, J Li, P Ma, Z Wang, W Shu, S Peng, GQ Chen: Chondrogenic differentiation of human bone marrow mesenchymal stem cells on polyhydroxyalkanoate (PHA) scaffolds coated with PHA granule binding protein PhaP fused with RGD peptide. Biomaterials 32: 2305-2313 (2011)
DOI: 10.1016/j.biomaterials.2010.12.009
PMid:21190731

26. Y Zhang, K Kumagai, T Saito: Effect of parathyroid hormone on early chondrogenic differentiation from mesenchymal stem cells. J Orthop Surg Res 9: 68 (2014)
DOI: 10.1186/s13018-014-0068-5
PMid:25079095 PMCid:PMC4237857

27. EA Makris, AH Gomoll, KN Malizos, JC Hu, KA Athanasiou: Repair and tissue engineering techniques for articular cartilage. Nat Rev Rheumatol 11: 21-34 (2015)
DOI: 10.1038/nrrheum.2014.157
PMid:25247412 PMCid:PMC4629810

28. JI Lee, M Sato, HW Kim, J Mochida: Transplantatation of scaffold-free spheroids composed of synovium-derived cells and chondrocytes for the treatment of cartilage defects of the knee. Eur Cell Mater 22: 275-90 (2011)
DOI: 10.22203/eCM.v022a21
PMid:22071698

29. M Vinci, S Gowan, F Boxall, L Patterson, M Zimmermann, W Court, C Lomas, M Mendiola, D Hardisson, SA Eccles: Advances in establishment and analysis of three-dimensional tumor spheroid-based functional assays for target validation and drug evaluation. BMC Biol 10: 29 (2012)
DOI: 10.1186/1741-7007-10-29
PMid:22439642 PMCid:PMC3349530

30. M Zanoni, F Piccinini, C Arienti, A Zamagni, S Santi, R Polico, A Bevilacqua, A Tesei: 3D tumor spheroid models for *in vitro* therapeutic screening: a systematic approach to enhance the biological relevance of data obtained. Sci Rep 6: 19103 (2016)
DOI: 10.1038/srep19103

PMid:26752500 PMCid:PMC4707510

31. MA Abboodi: Isolation, identification, and spheroids formation of breast cancer stem cells, therapeutics implications. Clinical Cancer Investigation Journal 3: 322 (2014)
DOI: 10.4103/2278-0513.134491

32. MJ Ware, K Colbert, V Keshishian, J Ho, SJ Corr, SA Curley, B Godin: Generation of Homogenous Three-Dimensional Pancreatic Cancer Cell Spheroids Using an Improved Hanging Drop Technique. Tissue Eng Part C Methods 22: 312-321 (2016)
DOI: 10.1089/ten.tec.2015.0280
PMid:26830354 PMCid:PMC4827286

33. X Gong, C Lin, J Cheng, J Su, H Zhao, T Liu, X Wen, P Zhao: Generation of Multicellular Tumor Spheroids with Microwell-Based Agarose Scaffolds for Drug Testing. PLoS One 10: e0130348 (2015)
DOI: 10.1371/journal.pone.0130348
PMid:26090664 PMCid:PMC4474551

34. P McMillen, SA Holley: Integration of cell-cell and cell-ECM adhesion in vertebrate morphogenesis. Curr Opin Cell Biol 36: 48-53 (2015)
DOI: 10.1016/j.ceb.2015.07.002
PMid:26189063 PMCid:PMC4639458

35. L Penolazzi, S Mazzitelli, R Vecchiatini, E Torreggiani, E Lambertini, S Johnson, SF Badylak, R Piva, C Nastruzzi: Human mesenchymal stem cells seeded on extracellular matrix-scaffold: viability and osteogenic potential. J Cell Physiol 227: 857-866 (2012)
DOI: 10.1002/jcp.22983
PMid:21830215

36. E Wright, MR Hargrave, J Christiansen, L Cooper, J Kun, T Evans, U Gangadharan, A Greenfield, P Koopman: The Sry-related gene Sox9 is expressed during chondrogenesis in mouse embryos. Nat Genet 9: 15-20 (1995)
DOI: 10.1038/ng0195-15
PMid:7704017

37. H Akiyama, MC Chaboissier, JF Martin, A Schedl, B de Crombrugghe: The transcription factor Sox9 has essential roles in successive steps of the chondrocyte differentiation pathway and is required for expression of Sox5 and Sox6. Genes Dev 16: 2813-2828 (2002)
DOI: 10.1101/gad.1017802
PMid:12414734 PMCid:PMC187468

38. DM Bell, KK Leung, SC Wheatley, LJ Ng, S Zhou, KW Ling, MH Sham, P Koopman, PP Tam, KS Cheah: SOX9 directly regulates the type-II collagen gene. Nat Genet 16: 174-178 (1997)
DOI: 10.1038/ng0697-174
PMid:9171829

39. P Smits, P Li, J Mandel, Z Zhang, JM Deng, RR Behringer, B de Crombrugghe, V Lefebvre: The transcription factors L-Sox5 and Sox6 are essential for cartilage formation. Dev Cell 1: 277-290 (2001)
DOI: 10.1016/S1534-5807(01)00003-X

40. V Lefebvre, W Huang, VR Harley, PN Goodfellow, B de Crombrugghe: SOX9 is a potent activator of the chondrocyte-specific enhancer of the pro alpha1 (II) collagen gene. Mol Cell Biol 17: 2336-2346 (1997)
DOI: 10.1128/MCB.17.4.2336
PMid:9121483 PMCid:PMC232082

41. P Zhang, SA Jimenez, DG Stokes: Regulation of human COL9A1 gene expression. Activation of the proximal promoter region by SOX9. J Biol Chem

278: 117-123 (2003)
DOI: 10.1074/jbc.M208049200
PMid:12399468

42. LC Bridgewater, V Lefebvre, B de Crombrugghe: Chondrocyte-specific enhancer elements in the Col11a2 gene resemble the Col2a1 tissue-specific enhancer. J Biol Chem 273: 14998-15006 (1998)
DOI: 10.1074/jbc.273.24.14998
PMid:9614107

43. I Sekiya, K Tsuji, P Koopman, H Watanabe, Y Yamada, K Shinomiya, A Nifuji, M Noda: SOX9 enhances aggrecan gene promoter/enhancer activity and is up-regulated by retinoic acid in a cartilage-derived cell line, TC6. J Biol Chem 275: 10738-10744 (2000)
DOI: 10.1074/jbc.275.15.10738
PMid:10753864

44. Q Zhao, H Eberspaecher, V Lefebvre, B De Crombrugghe: Parallel expression of Sox9 and Col2a1 in cells undergoing chondrogenesis. Dev Dyn 209: 377-386 (1997)
DOI: 10.1002/(SICI)1097-0177(199708)209:4<377::AID-AJA5>3.0.CO;2-F

45. M Kypriotou, M Fossard-Demoor, C Chadjichristos, C Ghayor, B de Crombrugghe, JP Pujol, P Galéra: SOX9 exerts a bifunctional effect on type II collagen gene (COL2A1) expression in chondrocytes depending on the differentiation state. DNA Cell Biol 22: 119-129 (2003)
DOI: 10.1089/104454903321515922
PMid:12713737

46. Z Chen, J Wei, J Zhu, W Liu, J Cui, H Li, F Chen: Chm-1 gene-modified bone marrow mesenchymal stem cells maintain the chondrogenic phenotype of tissue-engineered cartilage. Stem Cell Res Ther 7: 70 (2016)
DOI: 10.1186/s13287-016-0328-x
PMid:27150539 PMCid:PMC4858869

47. H Kitahara, T Hayami, K Tokunaga, N Endo, H Funaki, Y Yoshida, E Yaoita, T Yamamoto: Chondromodulin-I expression in rat articular cartilage. Arch Histol Cytol 66: 221-228 (2003)
DOI: 10.1679/aohc.66.221
PMid:14527163

48. K Nakata, H Nakahara, T Kimura, A Kojima, M Iwasaki, AI Caplan, K Ono: Collagen gene expression during chondrogenesis from chick periosteum-derived cells. FEBS Lett 299: 278-282 (1992)
DOI: 10.1016/0014-5793(92)80131-Y

49. M Ding, Y Lu, S Abbassi, F Li, X Li, Y Song, V Geoffroy, HJ Im, Q Zheng: Targeting Runx2 expression in hypertrophic chondrocytes impairs endochondral ossification during early skeletal development. J Cell Physiol 227: 3446-3456 (2012)
DOI: 10.1002/jcp.24045
PMid:22223437 PMCid:PMC3359397

50. G Musumeci, P Castrogiovanni, F Trovato, A Di Giunta, C Loreto, S Castorina: Microscopic and macroscopic anatomical features in healthy and osteoarthritic knee cartilage. OA Anatomy 1: 30 (2013)
DOI: 10.13172/2052-7829-1-3-898

Abbreviations: ADSCs: Adipose-derived stem cells, Acan: aggrecan, BSA: bovine serum albumin, Col1: collagen 1, Col2: collagen type II, ECM: extracellular matrix, MSCs: Mesenchymal stem cells, TBS: Tris-buffered saline

Key Words: Adipose-derived stem cells, Cartilage, Mesenchymal stem cells, Microtissue; Spheroids

Send correspondence to: Phuc Van Pham, Stem Cell Institute, VNU-HCM University of Science, 227 Nguyen Van Cu, District 5, Ho Chi Minh City 800010, Viet Nam, Tel: 84-28-36361206, Fax: 84-28-36361206, E-mail: pvphuc@hcmuns.edu.vn